Microbial Community Dynamics of a Sequentially Fed Anaerobic Digester Treating Solid Organic Waste

HyunWoo Lee[1,#], Temesgen M. Fitamo[1,#], Camila L. Nesbø[1], Nigel G. H. Guilford[1], Kärt Kanger[1,2], Minqing Ivy Yang[1], and Elizabeth A. Edwards[1]*

[#]These author (Lee and Fitamo) contributed equally to the work.

[1] Department of Chemical Engineering and Applied Chemistry and BioZone, University of Toronto, 200 College Street, Toronto, Ontario, Canada, M5S 3E5

[2] Faculty of Science and Technology, University of Tartu, Tartu, Estonia

*Corresponding author (EA Edwards)

Address correspondence to:

Elizabeth A. Edwards: elizabeth.edwards@utoronto.ca

Short title: Microbial community of solid-state anaerobic digestion of mixed organic waste

References formatted as Author-Date for ease of review; to be changed if accepted

Words: ~5785 (excluding abstract and references) + 5 figures

25 **Table of Contents (TOC)/ Abstract Art:**

26
27
28

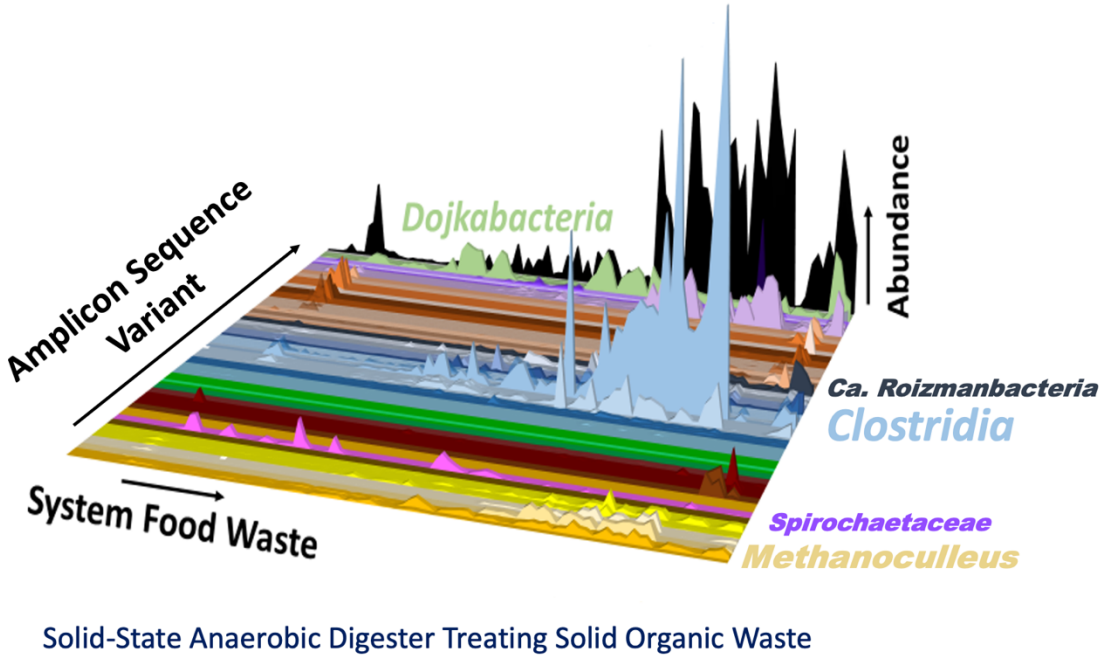

Solid-State Anaerobic Digester Treating Solid Organic Waste

29
30

31

32

33

34

35

36

37

38

39

Abstract

A 50 kg-scale high solids anaerobic digestor comprising six sequentially-fed leach beds with a leachate recirculation system and an upflow anaerobic sludge blanket reactor was operated at 37°C for 88 weeks. The feedstock contained a constant fibre fraction (a mix of cardboard, boxboard, newsprint, and fine paper) and varying proportions of food waste. Significantly enhanced co-digestion and methane production from the fibres was observed as the proportion of FW was increased. The most abundant 16S rRNA amplicon sequence variant (ASV), classified as *Clostridium butyricum*, was correlated with the amount of FW in the system and total methane yield. However, methane yield specifically from the fibre fraction was significantly correlated with organisms classified as *Candidatus Roizmanbacteria* and *Spirochaetaceae.* These ASVs together with ASVs classified as *Anaerovorax* and *Methanoculleus* correlated strongly to other ASVs in the microbial community, suggesting these are vitally important for ecosystem function and methane production. In addition, tracing the fate of microbes derived from incoming food waste helped to diagnose a poor batch of bulking agent.

Keywords: Anaerobic digestion, organic fraction municipal solid waste, 16S rRNA gene amplicon, microbial communities, synergy.

1. Introduction

Anaerobic digestion (AD) is commonly used for organic waste stabilization, mass reduction and renewable natural gas production. In anaerobic digestion, complex organics are converted into biogas mainly consisting of methane (CH_4) and carbon dioxide (CO_2). Biogas can be burned as a fuel or to generate heat and electricity or can be upgraded to pipeline quality and fed into natural gas grids. AD of the organic solids in municipal waste, referred to as Organic Fraction Municipal Solid Waste (OFMSW) is often not competitive with alternatives such as landfilling unless regulations limit such practices. As a result, in the U.S. and Canada, with more space and fewer landfill restrictions, a very large portion (75 million tons and 12 million tonnes respectively) of OFMSW ends up in landfills (Environment and Climate Change Canada, 2020; EPA, 2020).

The composition of OFMSW is heterogenous, variable and complex in nature. Conventional anaerobic digesters are preceded by extensive pre-treatment steps including size reduction, contaminant removal and dilution with water to make the feedstock suitable for pumping and further processing (Guilford et al., 2019). Continuous stirred tank reactors and plug flow reactors operating under mesophilic (37°C) or thermophilic (55°C) conditions effectively digest OFMSW (De Baere and Mattheeuws, 2013; Van et al., 2020). These wet-digestion configurations have been deployed in many cities, including Toronto (Gorrie, 2019) and many conventional digesters treating wastewater secondary bio-sludge are also now accepting pureed food waste (Chattha, 2020). High solids or so-called solid-state AD technologies (SS-AD) that enclose solid waste in silos or garage-type reactors (as reviewed in Li et al., 2011and others) can process more heterogeneous solids, but typically require longer residence times. To overcome the challenge of economic viability for OFMSW in the North

American context, Guilford et al. conceived of a modified SS-AD process inspired by landfill bioreactor technology (Guilford, 2009). In this new SS-AD design, OFMSW with minimal pre-treatment is placed sequentially in a series of 6 leach beds (one freshly fed leach bed per week), while leachate is recirculated to each location. A laboratory (50 Kg) scale demonstration system of this concept was built (affectionately known as "Daisy the Digester") and operated continuously for 88 weeks (Guilford et al., 2019). An important variable impacting digestion of OFMSW is the ratio of highly digestible Food Waste (FW) to other more slowly digested fractions, particularly paper and cardboard. Over the 88 weeks of operation the mass of fibre fed to Daisy remained constant, as did the proportions of its four constituents, fine paper (FP), boxboard (BB), cardboard (CB), and newsprint (NP). Over the same period, the mass of FW fed to Daisy varied from a low of 0 to a high of 29.3% of total chemical oxygen demand (COD) in the feed. The three major findings from this 88-week experiment (reported in Guilford et al., 2019) were that: 1) the addition of FW dramatically enhanced methane production from the paper and cardboard fibre fractions, and this enhancement was proportional to the amount of FW added; 2) observed total biogas yield at typical OFMSW composition (where ~29.3% of added COD is from FW) was as high as that achieved in well-mixed stirred tank reactors; and 3) the structure of the bulking agent used (wood chips in this case) impacted performance. Guilford *et al*. (2019) referred to the enhanced methane production from fibers by virtue of co-digestion of food wastes as "synergistic" methane production. Several factors likely contributed to this synergistic methane production, including greater microbial growth on FW, activity of hydrolytic enzymes in the FW, microbial community composition, biofilm formation, and leachate distribution and recirculation.

106 The main objective of this research was an analysis of the microbial community dynamics
107 in Daisy over this long-term experiment to try and explain the observed enhanced methane
108 production from the fibre fractions during co-digestion with food waste. Specifically, the goal
109 was to investigate links between the microbial community, process conditions and treatment
110 performance. This was achieved by (i) 16S rRNA amplicon sequencing to characterize the
111 microbial community in Daisy leachate over time, (ii) quantifying and identifying the most
112 abundant organisms using qPCR, (iii) correlating microbial community members with digester
113 performance parameters, particularly to methane production from fibres specifically, and (iv)
114 assessing functions of key microbes associated with enhanced methane production.
115

116 ## 2. Materials and Methods

117 ### 2.1 Solid state anaerobic digester configuration

118 The sequentially fed anaerobic leach bed configuration and feeding scheme are presented in
119 great detail in Guilford *et al*. (2019) and corresponding PhD thesis (Guilford, 2017). A brief
120 overview is provided here. A list of component and sample nomenclature for performance
121 metrics are provided in **Table S1** of the **supplementary information (SI).** Daisy the anaerobic
122 digester (**Figure S1**) consists of six leach beds (8.5 L working volume each), an up-flow sludge
123 blanket reactor (UASB, 27.5 L working volume), Tank 1 (UASB feed tank) and Tank 2 (leach
124 bed feed tank) each with a working volume of 17.5 L. The leach beds were sequentially batch
125 fed at one-week intervals. The temperature in the tanks and the UASB was controlled at 37^{o}C.
126 The leachate was continuously recirculated and successively delivered to each of the leach
127 beds using a leach bed feed pump and control valves (**Figure S1**). Leach beds received 560 ml
128 of leachate every 30 minutes. Leachate was collected in Tank 1. The content of Tank 1 was

pumped to the UASB and the effluent from the UASB was recycled to Tank 2. Pump 2 was used to maintain hydraulic balance between Tank 1 and Tank 2. Refer to Guilford *et al*. (2019) for additional information.

2.2 Feedstock preparation and digester operation

The feedstock composition was designed to simulate an average typical mixed organic solid waste sent to landfill, which in Canada contains about 38% (wet weight) FW and 62% lignocellulosic (i.e. paper and cardboard) fibres (Mcintyre, 2007; Statistics Canada, 2010). Expressed as COD, this typical composition translates to ~17.2% COD from FW; this proportion was used as the base case in these experiments. All wastes were collected from residential waste recycling programs in Greater Toronto. The source-separated FW was shredded to less than 10 cm and stored frozen in individual bags at -20^{o}C until use. A defined fibre blend of shredded FP, BB, CB, and NP was also prepared. Bulking agent (BA) prepared by the recycling facility from shredded ash wood was mixed into the feedstock mixture to maintain hydraulic permeability during digestion. Eight batches of BA were received over the course of 88 weeks of reactor operation.

The digester (**Figure S1**) was inoculated with anaerobic digester sludge from a pulp and paper mill. Each week, the oldest of the 6 leach beds in the system was replaced with a new leach bed containing fresh feed, providing a solids retention time (SRT) of six weeks. The system was operated for 88 weeks, divided into 12 periods, each period defined by a change in operation, primarily the quantity of FW added, as summarized in **Table S2a**. Initially, the proportion of FW added was 17.2% on a COD basis, which was subsequently decreased in 3 stages to zero, then increased back up to 17.2% in one step, further increased to 21.7%, and

ultimately to 29.3% COD of FW in the final stage of operation (details in **Tables S2b & S2c**). The source, mass and composition of the fibre mixture added to each leach bed remained constant throughout as did the mass of BA (wood chips). All the waste samples were received in several batches over time.

2.3 Sample collection and preservation for microbial analysis

Between weeks 31 and 88, leachate samples were taken for DNA extraction (**Table S2d**) and eventual microbial analysis from nine ports across the reactor. These samples were collected weekly from all leach-beds, six hours after completing the installation of a new leach bed in one of the 6 leach bed locations (LL). Duplicate leachate samples (10 mL each) were collected from valves (V1-1 to V1-6) located directly below each leach bed, as well as from Tanks 1 & 2 and the UASB, as shown in **Figure S1**. Each week, one additional sample called the "first flush" (labelled W0) was collected from the newly installed leach bed right after installation to capture the first liquid displaced out of the waste. Samples were labeled according to the leach bed serial number and the corresponding time in Daisy, or SRT. As an example, referring to **Figure S2 (which is a close-up of Table S2b)**, leach bed number serial number S.031 was installed in leach bed location #1 (LL01) on 10/27/2015 for six-weeks (weeks 32 to 37) before it was replaced by a new leach bed (S.037). The first flush sample taken right after installation of leach bed S.031 was labeled S31W0. The next sample was taken six hours later and labeled S31W1. Subsequent samples taken at exactly weekly intervals are labelled S31W2 to S31W6.

A slight change in leachate sampling workflow occurred at week 61. Prior to week 61, samples (10 mL) were collected in falcon tubes and directly placed in a -20^{o}C freezer for later DNA extraction. However, after week 61, samples (10 mL) were first centrifuged at 7000Xg at 4^{o}C

for 30 minutes (Beckman Coulter Avanti J-E Series, JLA 16.250 fixed angle rotor) and most of the supernatant was discarded. The pellets were resuspended in the 1 mL remaining supernatant and transferred to a 2 mL Safe-seal Micro Tube (Sarstedt) and further centrifuged at 13,000Xg for 15 minutes (Eppendorf Microcentrifuge 5417R). The supernatant was removed, and the pellets were stored at -80 °C for later DNA extraction. The DNA extraction method was the same for both sets of samples. A total of 111 leach bed leachate samples were collected (**Tables S2d and S3**). The samples corresponded to the first and the last leach bed of each operating period, chosen because the first leach bed reflected the immediate impact of a change in FW COD added while the last leach bed corresponded to when all six leach beds were fed same ratio of fibres to FW. First flush samples (W0) provided an estimate of the microbial community in the feed. Samples for DNA extraction were also collected from the original inoculum to Daisy (seed), from samples of FW used as feedstock, and from the feedstock mix comprised of a mix of FW and fibres. Finally, samples were also taken from 6-week-old digestate (DG), and from the sludge in the bottom of Tank 1, Tank 2 and the UASB upon decommissioning after week 88 (**Table S3).**

2.4 DNA Extraction and Quantitative Polymerase Chain Reaction (qPCR)

DNA extractions from leachate were performed using the Qiagen DNeasy PowerSoil kit (Qiagen, Carlsbad, CA) according to the manufacturer's protocol with the following modifications: (i) instead of transferring the recommended volume of sample through step 9 to 15, the entire supernatant volume was transferred for quantitative analysis and (ii) DNase- and RNase-free sterile water (Invitrogen) was used for elution instead of C6 elution buffer provided in the kit to minimize interference in downstream molecular analysis. DNA extractions from FW, leach bed feedstock mix, and DG were performed using Qiagen DNeasy

196 PowerMax DNA isolation kit according to the kit protocol. The extracted DNA from the FW,
197 leach bed feedstock mix and DGs, nine samples in total, were further concentrated with 100%
198 ethanol and 5 M NaCl prior to sequencing (Kanger et al., 2020). The final DNA concentration
199 was measured by Nanodrop (NanoDrop1000 Spectrophotometer, Thermo Fisher Scientific).
200 The absolute abundance of bacteria and archaea was determined using quantitative PCR
201 (qPCR) with primers targeting bacterial or archaeal 16S rRNA genes as explained and
202 provided in **Table S4**. Raw qPCR data are provided in **Tables S5a** (bacteria) and **S5b**
203 (archaea).

204 **2.5 Amplicon and Shotgun Sequencing and Data Analysis**

205 DNA extracts were sent to the McGill University and Genome Quebec Innovation Center
206 (Quebec, Canada) for amplicon sequencing using the Illumina MiSeq system and the V3
207 reagent kit with primers targeting the V6-V8 regions of the 16S rRNA gene, with sequences
208 926f-modified: 5'-AAACTYAAAKGAATWGRCGG-3' and 1392r-modified: 5'-
209 ACGGGCGGTGWGTRC-3' (Qiao et al., 2020). The raw amplicon sequence data were
210 submitted to the National Centre for Biotechnology Information's (NCBI) sequence read
211 archive (SRA) database under Bio-Project PRJNA501900. Shotgun metagenomes of select
212 DNA samples from Daisy were also previously sequenced using Illumina technology as
213 described in Kanger et al., 2020, and this data is available in the Joint Genome Institute GOLD
214 database under Gs0130338, study name: metagenomes from anaerobic digester of solid waste.

215 The raw amplicon sequences obtained from Genome Quebec were processed and
216 analyzed using QIIME2 version 2019.10 (Bolyen et al., 2019). After trimming the primer
217 region with the cutadapt plug-in, amplicon sequence variants (ASVs) were generated using the

DADA2 plug-in with the following settings: p-trunc-len-f = 260, p-trunc-len-r = 240 or 220 bp, p-max-ee = 2. The amplicon sequencing summary statistics are provided in **Table S6**. The resulting data set was subsampled to an equal depth of 14,900 reads per sample prior to analysis to minimize the bias caused by different read-depth. Taxonomic classification was performed using the Silva-132-99-nb classifier trained on the 926f and 1392r primer set. All ASVs, corresponding sequences, and taxonomic classifications are provided in **Table S7**.

The V6-V8 primers recover both bacterial and archaeal sequences, as well as some 18S sequences from eukaryotes. The relative abundance of ASVs in each domain was calculated by dividing number of reads for a given bacterial ASV by the total number of bacterial reads, repeated for archaeal reads (**Table S7**). For graphing, genera with > 5% relative abundance in any sample were identified and grouped while the remaining ASVs were clustered together as "Others" (**Table S8)** and the resulting bar graph for all leachate samples is provided in **Figure S13**. Finally, the absolute abundance of each ASV was estimated by multiplying bacterial or archaeal relative abundance by the total bacterial or archaeal abundance measured by qPCR (**Table S9**).

2.6 Measurements of Process Parameters and Reactor Performance

A detailed account of the many process parameters measured in Daisy was previously reported, including biogas and methane production, and leachate analyses for total and volatile solids (TS/VS), COD, pH, alkalinity ratio, volatile fatty acids (VFAs), sulfate, and inorganic salt concentrations (Guilford *et al*., 2019). The total volume of biogas produced was continuously measured using two independent wet-tip gas meters, one serving the leach beds and tanks combined and the other the UASB alone. Biogas composition was analyzed regularly, and

240 volumes converted to methane at STP. The methane produced specifically from the fibres (**FB-**
241 **Methane**) was calculated as the total methane produced minus the maximum possible methane
242 that could be produced from added FW assuming 78% COD_{FW} conversion (**Figure S3** and
243 **Table S10**). The 78% maximum conversion efficiency for FW COD was verified in
244 independent biochemical methane potential tests (Guilford *et al*., 2019).

245 **2.7 Correlation and statistical Analyses**

246 Both the relative abundance and the absolute abundance of microbial taxa were analyzed using
247 the Phyloseq package V1.26 (McMurdie and Holmes, 2013) in R (R Core Team, 2013).
248 Ordination analyses were performed using Non-Metric Multidimensional scaling (NMDS) on
249 Bray-Curtis distances calculated from the absolute or relative abundance data. All available
250 operating and measured process variables were included as metadata (**Table S11**). A network
251 of 100 ASVs with highest absolute abundance and metadata was constructed using the CoNet
252 application in Cytoscape (Faust and Raes, 2016) and the co-occurrence network model was
253 displayed with Cytoscape 3.7 (Shannon et al., 2003). Four methods were used to assess the
254 relationship between ASVs and metadata: Bray Curtis distances, Mutual information, Pearson,
255 and Spearman correlations, and three methods were required to support each edge (lines
256 connecting ASVs and metadata in the network diagram). Significance of the edges was
257 assessed using the combination of permutations and bootstrapping described in Faust and Raes
258 (2016). The initial network contained 1,000 positive and 1,000 negative edges consistent
259 across all four correlation measures. For each measure and each edge, 1,000 renormalized
260 permutation and bootstrap scores were generated. P-values for each method were merged and
261 edges with a false discovery rate (FDR) value < 0.01 were retained. In a second, more stringent
262 analysis, the p-values were not merged for each method before retaining edges with FDR <

0.01, and three methods were required to support each edge. Generalized Linear Model (GLM) analysis was performed in SAS studio 3.8 (SAS version 9.04, 2018) to visualize the correlation of the 100 most abundant ASVs using absolute abundance and process metadata. The ASVs were considered as traits and analyzed separately but iteratively with the GLM. Bonferroni adjustment method was used to make correction for multiple comparisons (Aickin and Gensler, 1996; Bender and Lange, 2001).

3. Results and Discussion

3.1 Overview of system performance and associated microbial community shifts

Amplicon sequencing of the SSU rRNA gene was conducted on 131 samples from Daisy as the amount and proportion of FW was varied (**Table S3**). A total of 7466 ASVs were identified (**Table S7).** System performance and underlying leachate microbial community profiles are illustrated in **Figure 1**. Biogas production (red line) tracked the amount of FW fed to Daisy (green line) as a function of time (in weeks) overlaying corresponding microbial community profiles (relative abundance) from weekly representative leachate samples, omitting first flush samples. Each leach bed received a constant amount of fibre, which comprised the majority of the COD added, and the basal gas produced at 0 %FW (weeks 46-49) is from digestion of fibres alone. The microbial community sampled weekly was reproducible and shifted progressively as the %FW in the system changed. Given that leachate is recirculated to all leach beds regardless of their age, the data do show that good mixing is occurring in the system, despite the stationary nature of the solid substrates. The microbial community composition was found to be very different when no FW was added, seemingly to be more enriched in Candidatus *Dojkabacteria* (previously referred to as WS6) (green bars in **Fig.1**),

286 *Kineosporiaceae* (pink bars), and methanogens (yellow bars), while at high FW, the
287 community was dominated by *Clostridia* and *Spirochaetacea* (Blue and purple bars in **Fig. 1**).
288 Samples of the inoculum and of the food waste before digestion were also analyzed (**Figure**
289 **S4**). Microbes derived from food waste (mainly *gamma proteobacteria* shown in brown
290 shades) were only present in "first flush" samples corresponding to the first liquid drained
291 from a newly installed leach bed (**Figure S5)** and in leachate samples during a period of
292 unexpectedly poor performance (low biogas production; weeks 61-63 in **Figure 1**), previously
293 attributed to the use of a batch of BA with a different morphology (Batch #5) during this time
294 (Period 5b: "Odd BA" Guilford, 2019). Other than during this period, the microbial phylotypes
295 detected in the leachate samples all originated from the original pulp mill inoculum and not
296 from the food waste (**Figure S4**). None of the microbes from food waste were found to
297 proliferate in Daisy, consistent with our previous study of antimicrobial genes in Daisy
298 (Kanger et al., 2020). This overview of the microbial data prompted a deeper investigation of
299 the relationships between the microbial community and process parameters.
300

301 **3.2 Most abundant taxa illustrating a pitfall of relative abundance estimates**

302 Absolute microbial abundance measurements are more relevant to understanding process
303 kinetics because the rate of reaction is proportional to biomass concentrations. The absolute
304 abundance of each bacterial and archaeal phylotype was calculated using qPCR measured
305 bacterial and archaeal total abundances combined with relative abundance data from amplicon
306 sequencing. **Figure 1** re-plotted using absolute abundance of bacteria (**Figure S6a**) and
307 archaea (**Figure S6b**). These plots clearly show that absolute abundance of both total bacteria
308 and total archaea track methane production and FW proportion very closely. Strikingly, in this

309 view, the seemingly high relative abundance of *Djokobacteria* (green bars) observed when
310 there was little FW in the system really corresponded to low absolute numbers of these
311 organisms. In fact, the absolute abundance of *Djokobacteria* does not change much with
312 changing process conditions (**Figure S6a**). This observation illustrates a common pitfall when
313 relying only on relative abundance profiles.

314 The most abundant bacterial taxa, based on qPCR and amplicon data, belonged to the
315 class *Clostridia (*1860 ASVs*)* and the *Spirochaetia (*382 ASVs*)*, together accounting for more
316 than 50% of the bacterial community **(Figure S6a).** *Methanosaeta*, *Methanolinea*,
317 *Methanoculleus* and *Methanobacterium* were the most abundant archaeal genera (**Figure**
318 **S6b).** The microbial communities of the sludge from the tanks and UASB and the DG at high
319 FW were also dominated by methanogens that seem to be in higher abundance in sludge and
320 digestate than in leachate (**Figure S7).** The data also revealed a shift in the methanogenic
321 community from *Methanobacterium* at low % FWCOD to a more diverse community at higher
322 % FW COD including acetoclastic *Methanosaeta* and hydrogenotrophic *Methanoculleus*.
323 Given that the amplicon primers used to capture both eukaryotic and prokaryotic sequences,
324 the FW also comprised 10-25% of plant-derived sequences (**Figure S4**), including both plant
325 18S rRNA sequences and 16S rRNA sequences associated with *Chloroplast*s. The remainder
326 comprised 16S rRNA sequences attributed to various *Gammaproteobacteria.* Archaea were
327 absent in these feed samples.

328 Although more informative, quantitative data from qPCR still does not accurately
329 reflect the mass of the respective cell types because cell size and number of 16S rRNA genes
330 per genome are not considered. The observed order of magnitude higher copies for total

bacteria relative to total archaea (**Figures S6a vs S6b**) most likely reflects that Clostridia have an average 10 copies of the 16S rRNA gene per cell while methanogens average only 1 to 2 copies per cell (Stoddard et al., 2015).

3.3 Ordination analysis

NMDS ordinations were performed for all ASVs using both absolute and relative abundance data and the results are shown in **Figure 2** and **Figure S8,** respectively. While both ordinations showed similar clustering, the ordination based on absolute abundances was chosen for greater relevance to process parameters. The NMDS ordination (**Figure 2)** revealed that samples clustered along the X-axis from right (orange) to left (grey) as digestion progressed. Samples further clustered according to % FW COD added along the Y-axis from the bottom (no FW; pale blue) to the top (high FW; dark green). The microbial communities of "first flush" samples (ending with W0), collected from each new leach bed upon installation, clustered closest to those in FW samples. A unique set of data, coloured in pink in **Figure 2,** correspond to samples from the period with poor performance related to BA Batch #5 and are further discussed below. The same ordination, coloured instead by weeks of digestion (i.e., solids retention time or SRT), is shown in **Figure S9**. In this view, samples taken six hours after feeding (ending with W1) to samples collected at week 6 (ending with W6), are distributed from right to left according to SRT and from bottom to top according to % FW. Overall, these data illustrate the very tight connection between the microbial communities in the leach bed leachate and process operating conditions.

3.4 Impact of bulking agent (BA)

By week 57, the supply of BA Batch #4 was running low, and so Batch #5 was used. As reported in Guilford et al., (2019), digester performance immediately began to decline, as can be seen by the drop in biogas production, particularly during weeks 61-63 (**Figure 1**; BA Batch #5 period). The drop in performance was attributed to the physical properties of the particular batch of BA, specifically morphology, since no other changes had been made. Performance was restored by reverting to Batch #4, followed by Batch #6 (with similar specifications as Batch #4) (**Figure S10**). Why did BA#5 have such an impact? As noted previously, a significant difference in the microbial composition of leachate samples coincided with this period. These leachate samples contained significant proportions of FW-derived microbes, even after many weeks of digestion (**Figure S5**). This can also be seen in the NMDS ordination (**Figure 2**) where BA#5 samples clustered more closely to flush and FW samples, regardless of their SRT**.** The community composition reverted to a more typical composition when the BA was changed back (**Figure S5**). The shorter and coarser features of BA#5 (**Figure S10**) not only resulted in higher permeability and lower water retention, but clearly also impacted the microbial community, which in turn affected performance. Specifically, the higher permeability likely resulted in greater channelling within the leached solids and less effective distribution of recirculating leachate, explaining why FW derived microbes could still be seen in samples of leachate even after 3, 4 or 5 weeks (**Figure S5**). These data highlight the importance of the BA and associated hydrodynamics for adequate performance of high solids digesters. While the impact of BA#5 was reversible and the bacterial community rebounded, it seemed to have caused in a shift in dominant hydrogenotrophic methanogens from *Methanobacterium* to *Methanoculleus* over this period.

3.5 Which organisms correlate to enhanced biogas production from fibres?

Guilford et al., (2019) observed that the addition of FW to Daisy greatly enhanced methane production from fibre fractions and referred to this observation as "synergy" (**Figure 3**). To investigate the relationship between microbial community composition and methane production from FW and from fibres, a co-occurrence network of the 100 most abundant ASVs **(Table S9)** and the entire set of process metadata **(Table S11)** was constructed for the leachate samples. The full network, with edges supported by at least three of four correlation methods used and a merged false discover rate (FDR) < 0.01, is shown in **Figure S11**. Concentrations of VFAs and sulfate, and pH and alkalinity ratio were not correlated with community composition, consistent with these being stable throughout the experimental period. In contrast, metadata related to methane production and amount of FW in the system were significantly correlated with ASVs (**Figure S11**). These metadata included total methane (liters per week), overall methane yield (L Methane /kg COD added), methane yield specifically from fibres (L methane from fibres/kg FBCOD added, labeled FB-Methane Yield) and total system FW (i.e., the sum of FW COD in the 6 installed leach beds at time of sampling, labeled FW6LB). A subnetwork shown in **Figure 4A** was constructed including only the eleven ASVs that were significantly correlated with process metadata. Among these ASVs, eight were correlated with FB-methane yield: *Clostridium butyricum* (ASV4124), *Clostridium* sensu stricto 1 (ASV4109), *Anaerovorax* (ASV2339), *Spirochaetaceae* (ASV596), *Candidatus Roizmanbacteria* (ASV6579 and ASV6584), *Methanosarcina* (ASV6270), and *Methanoculleus* (ASV6332). All eight ASVs were also correlated with the amount of FW available in the system. Moreover, *Anaerovorax* (ASV2339), *Spirochaetaceae* (ASV596), *Candidatus Roizmanbacteria* (ASV6584) and *Methanoculleus* (ASV6332) were the ASVs

399 with highest number of positive connections in the full network (50-43 positive connections
400 compared to an average of 18), suggesting they may also be hub-species important for
401 ecosystem structure and function (Bussi and Gutierrez, 2019).

402 A more stringent subnetwork (**Figure 4B)** was created where at least three correlation
403 measures must be significant based on unmerged or individual FDR-values. The highly
404 abundant *Clostridium butyricum* ASV (ASV4124), which was significantly correlated to all
405 four metadata categories in **Figure 4A**, only correlated with FW in the system and total
406 methane but not with FB-methane yield or overall methane yield in **Figure 4B**. In this more
407 stringent network, only *Spirochaetaceae* (ASV596) and *Candidatus Roizmanbacteria*
408 (ASV6579) were correlated specifically with FB-Methane yield. This more stringent network
409 also reveals most significant correlations between ASVs, discussed in Section 3.6.

410 The correlation between the microbial populations identified in the network analysis
411 and FB-methane yield were further examined and validated using GLMs (**Table S12).** These
412 analyses confirmed a strong correlation between the set of organisms identified in the network
413 and FB-Methane Yield (Pearson correlation r 0.70 - 0.83) (**Figure 5 and Figure S12**).
414 Interestingly, the ASV with the highest correlation coefficient was *Candidatus*
415 *Roizmanbacteria* (ASV6584) (**Figure 5**), suggesting that this phylotype may be particularly
416 important for conversion of fibres to methane in the presence of food waste. Finally,
417 confirming early observations based on qPCR abundances, Candidatus *Dojkabacteria* (WS6)
418 shows very poor correlation with FB-Methane Yield or food waste in Daisy (**Figure 5**).

419

3.6 Ascribing roles to major microorganisms in Daisy

Not surprisingly, *Firmicutes,* particularly *Clostridiales*, were present in high relative and absolute abundances in Daisy, re-affirming their importance in solid waste digestion. *Firmicutes* often produce lipases, proteases, and other extracellular enzymes to facilitate hydrolysis and acidogenesis (Leven et al., 2007; Rintala and Puhakka, 1994). *Clostridia* are often reported as important microbes in AD, for example in reactors treating organic household wastes (Cardinali-Rezende et al., 2009) and corn straw (Qiao et al., 2013). The ASV classified as *C. butyricum* (ASV4124) was the most abundant bacterial lineage in most leachate samples, accounting for as much as 70% of the community at the highest loading of FW COD (sample S81W1). The abundance of *C. butyricum* ASV4124 is likely overestimated by at least a factor of 2 relative to other bacteria, as strains of this organism contain 8-12 rRNA copies in their genome (Mo et al., 2015; Stoddard et al., 2015), more than twice of the average copy number (i.e., 4.2) observed for bacteria (Větrovský and Baldrian, 2013). *C. butyricum* are fermenters known to produce hydrogen and organic acids during degradation of organic substrates, especially carbohydrates (Liu et al., 2012). In agreement with this, the network analyses suggested that *C. butyricum* ASV4124 was significantly correlated with FW, even when applying the most stringent correlation criteria (**Figure 4B**). Therefore, we hypothesize that *C. butyricum* ASV4124 was mainly growing on the FW, and perhaps not the lignocellulose fibres in the feed.

Several candidate taxa were also prominent in the Daisy microbiome. Two ASVs annotated to *Candidatus Roizmanbacteria (*ASV6579, ASV6584) were significantly correlated with all bioprocess metadata (**Figure 4A**), and ASV6579 was one of the only two ASVs significantly correlated with FB-methane yield in the most stringent network (**Figure**

443 **4B)**. Moreover, both *Ca. Roizmanbacteria* ASVs showed high levels of connection to other
444 ASVs, i.e., with 45 and 28 connections in the full network **(Figure S11).** *Ca. Roizmanbacteria*
445 have been suggested to be symbionts, capable of metabolizing various complex carbon
446 substrates such as cellulose and have also been reported to be involved in lipid metabolism and
447 to produce lactate for other microorganisms (Campanaro et al., 2019; Geesink et al., 2020).
448 Geesink et al., 2020 suggested that these bacteria, in addition to plant materials, also utilize
449 dead microbial biomass. Thus, in the Daisy ecosystem *Ca. Roizmanbacteria* are likely
450 important 'connecting' organisms, producing lactate and degrading cellulose and dead cell
451 biomass.

452 The ASV annotated as *Spirochaetaceae* (ASV596) was also connected to FB-methane
453 yield and system FW (FW6LB) (**Figures 4A and 4B)** and was the ASV with the most
454 connections in the overall network (52 connections, supplemental **Figure S11**). Thus, these
455 *Spirochaetaceae* appear to provide essential functions in the Daisy microbial community and
456 possibly in the synergistic FB-methane production. *Spirochaetaceae* have been observed in
457 anaerobic digesters treating sludge (Chouari et al., 2005) and digester fed with starch, glucose,
458 ethanol, lactate, acetate, propionate, butyrate, succinate, and formate (Delbès et al., 2000).
459 S*pirochaetes* have been suggested to be involved in syntrophic acetate oxidation in anaerobic
460 digesters in association with hydrogenotrophic methanogenesis (Lee et al., 2015, 2013). Fibre-
461 associated *Spirochaetes* were also reported to be major hemicellulose degraders in hindgut of
462 wood-feeding higher termites (Tokuda et al., 2018). The strong correlation of *Spirochaetaceae*
463 ASV596 with FB-methane yield (**Figure 5**) suggests that they may also be capable of
464 degradation and use of lignocellulosic fibres and produce acetate, H_2 and CO_2 to facilitate
465 syntrophic methane production. Shotgun metagenome sequencing was performed on select

samples (**Table S3**). The analysis of metagenome-assembled genomes (MAGs) from Daisy is out of the scope of this paper, but a preliminary survey of possible MAGs for *Ca. Roizmanbacteria and Spirochaetaceae* revealed many genes for cellulose degradation and other carbohydrate active enzymes, consistent with these correlations.

Two archaeal ASVs, annotated as *Methanoculleus* (ASV6332) and *Methanosarcina* (ASV6270), were significantly correlated with FB-methane yield (**Figure 4A**). *Methanosarcina* are versatile methanogens that utilize acetoclastic, hydrogenotrophic and methylotrophic methanogenesis pathways for growth and methane production (Singh et al., 2005; Sowers et al., 1984; Town and Dumonceaux, 2016; Von Klein et al., 2002). *Methanoculleus* metabolize formate, alcohols, and H_2/CO_2 to methane and usually require acetate as carbon source (Chen et al., 2015; Dianou et al., 2001; Lai, 2019; Maus et al., 2012). In the more stringent network in **Figure 4B**, two *Methanoculleus* ASVs (ASV6332 and ASV6331) are connected to *Spirochaetaceae* ASV596, suggesting a possible syntrophic relationship between these organisms. The different methanogens revealed in the networks of Figure 4 are known to make use a variety of substrates and likely contributed to the stability of Daisy by consuming H_2, acetate and formate and making otherwise difficult fermentations thermodynamically possible. In particular, the close relationship between *Spirochaetaceae* and *Methanoculleus* suggests metabolites produced by *Spirochaetaceae,* during degradation are consumed by *Methanoculleus*. We observed that Daisy was remarkably stable even at elevated FW COD added and never experienced build-up of volatile fatty acids or pH upset. We also noted that *Methanobacterium* were prevalent at lower food waste while *Methanoculleus* became abundant at higher food waste. This switch also occurred around the time of the odd bulking agent.

ASVs classified as *Candidatus Dojkabacteria*, particularly ASV6777, did not show significant correlation to methane production or how much food waste was added to Daisy in our network analysis (**Figure 5);** yet as previously noted, were present at high relative abundance at low FW. Cand. *Dojkabacteria* have been observed in digesters treating corn straw (Qiao et al., 2011), sewage sludge (Liu et al., 2016) and swine sludge (Cardinali-Rezende et al., 2012), yet their function is not known. They have been shown to encode form II/III RubisCO genes used in light independent CO_2 incorporation into sugars derived from nucleotides (Wrighton et al., 2016). Based on literature findings and our data, we proposed that these organisms in Daisy are well adapted to persisting at low nutrient levels such as with limited FW.

4. Conclusion

Enhanced production of methane from lignocellulosics fibres when co-digested with food waste (termed "synergistic" methane production) was linked to an order of magnitude or more increase in absolute microbial abundance as food waste proportion increased. Moreover, very specific microbial taxa (ASVs) were implicated via multiple analyses. These taxa connected all of the digestion stages from hydrolysis, through various fermentations to methanogenesis. The community became progressively and stably enriched in these taxa as food waste increased. Most significant phylotypes at higher food waste included hydrolytic and fermentative bacteria from *Clostridium* sensu stricto particularly *Clostridium butyricum*, *Anaerovorax*, *Candidatus Roizmanbacteria*, and *Spirochaetaceae* in association with *Methanoculleus* and *Methanosarcina*. The robustness of the microbial community and associated digestion process is well illustrated by how quickly performance rebounded

following a period of bad bulking agent, and by the high overall methane yield obtained in this high-solids anaerobic digestion configuration treating typical organics from municipal waste.

5. Acknowledgements

This research was funded by the Natural Sciences and Engineering Research Council of Canada (Collaborative Research and Development Grant) and by Miller Waste Systems Inc. We thank Charlie Cassin of Miller Waste Systems for preparing and providing feed samples. We thank Cristina Sartori (Researcher at University of Padova, Italy) for providing training in GLM analysis. We thank Shen Guo, Endang Susilawati, Line Lomheim and Vinthiya Paramananthasivam (BioZone, University of Toronto) for providing technical and administrative support during this extensive research project.

6. References

Aickin, M., Gensler, H., 1996. Adjusting for multiple testing when reporting research results: The Bonferroni vs Holm methods. Am. J. Public Health 86, 726–728. https://doi.org/10.2105/AJPH.86.5.726

Bender, R., Lange, S., 2001. Adjusting for multiple testing - When and how? J. Clin. Epidemiol. 54, 343–349. https://doi.org/10.1016/S0895-4356(00)00314-0

Bolyen, E., Rideout, J.R., Dillon, M.R., Bokulich, N.A., Abnet, C.C., Al-Ghalith, G.A., Alexander, H., Alm, E.J., Arumugam, M., Asnicar, F., Bai, Y., Bisanz, J.E., Bittinger, K., Brejnrod, A., Brislawn, C.J., Brown, C.T., Callahan, B.J., Caraballo-Rodríguez, A.M., Chase, J., Cope, E.K., Da Silva, R., Diener, C., Dorrestein, P.C., Douglas, G.M., Durall, D.M., Duvallet, C., Edwardson, C.F., Ernst, M., Estaki, M., Fouquier, J., Gauglitz, J.M., Gibbons, S.M., Gibson, D.L., Gonzalez, A., Gorlick, K., Guo, J., Hillmann, B., Holmes, S., Holste, H., Huttenhower, C., Huttley, G.A., Janssen, S., Jarmusch, A.K., Jiang, L., Kaehler, B.D., Kang, K. Bin, Keefe, C.R., Keim, P., Kelley, S.T., Knights, D., Koester, I., Kosciolek, T., Kreps, J., Langille, M.G.I., Lee, J., Ley, R., Liu, Y.X., Loftfield, E., Lozupone, C., Maher, M., Marotz, C., Martin, B.D., McDonald, D., McIver, L.J., Melnik, A. V., Metcalf, J.L., Morgan, S.C., Morton, J.T., Naimey, A.T., Navas-Molina, J.A., Nothias, L.F., Orchanian, S.B., Pearson, T., Peoples, S.L., Petras, D., Preuss, M.L., Pruesse, E., Rasmussen, L.B., Rivers, A., Robeson, M.S.,

542 Rosenthal, P., Segata, N., Shaffer, M., Shiffer, A., Sinha, R., Song, S.J., Spear, J.R.,
543 Swafford, A.D., Thompson, L.R., Torres, P.J., Trinh, P., Tripathi, A., Turnbaugh, P.J.,
544 Ul-Hasan, S., van der Hooft, J.J.J., Vargas, F., Vázquez-Baeza, Y., Vogtmann, E., von
545 Hippel, M., Walters, W., Wan, Y., Wang, M., Warren, J., Weber, K.C., Williamson,
546 C.H.D., Willis, A.D., Xu, Z.Z., Zaneveld, J.R., Zhang, Y., Zhu, Q., Knight, R.,
547 Caporaso, J.G., 2019. Reproducible, interactive, scalable and extensible microbiome
548 data science using QIIME 2. Nat. Biotechnol. https://doi.org/10.1038/s41587-019-0209-
549 9
550 Bussi, C., Gutierrez, M.G., 2019. From hairballs to hypotheses–biological insights from
551 microbial networks. FEMS Microbiol. Rev. 43, 341–361.
552 https://doi.org/10.1093/FEMSRE
553 Campanaro, S., Treu, L., Rodriguez-R, L., Kovalovszki, A., Ziels, R., Maus, I., Zhu, X.,
554 Kougias, P., Basile, A., Luo, G., Schlüter, A., Konstantinidis, K., Angelidaki, I., 2019.
555 The anaerobic digestion microbiome: a collection of 1600 metagenome-assembled
556 genomes shows high species diversity related to methane production. Anaerob. Dig.
557 microbiome a Collect. 1600 metagenome-assembled genomes shows high species
558 Divers. Relat. to methane Prod. 680553. https://doi.org/10.1101/680553
559 Cardinali-Rezende, J., Debarry, R.B., Colturato, L.F.D.B., Carneiro, E. V., Chartone-Souza,
560 E., Nascimento, A.M.A., 2009. Molecular identification and dynamics of microbial
561 communities in reactor treating organic household waste. Appl. Microbiol. Biotechnol.
562 84, 777–789. https://doi.org/10.1007/s00253-009-2071-z
563 Cardinali-Rezende, J., Pereira, Z.L., Sanz, J.L., Chartone-Souza, E., Nascimento, A.M.A.,
564 2012. Bacterial and archaeal phylogenetic diversity associated with swine sludge from
565 an anaerobic treatment lagoon. World J. Microbiol. Biotechnol. 28, 3187–3195.
566 https://doi.org/10.1007/s11274-012-1129-8
567 Chattha, S., 2020. Municipal Co-digestion—How a Provincial-Scale Initiative is Helping
568 Reduce GHG Emissions [WWW Document]. URL
569 https://www.watercanada.net/feature/municipal-co-digestion-how-a-provincial-scale-
570 initiative-is-helping-reduce-ghg-emissions/ (accessed 11.17.21).
571 Chen, S.C., Chen, M.F., Lai, M.C., Weng, C.Y., Wu, S.Y., Lin, S., Yang, T.F., Chen, P.C.,
572 2015. Methanoculleus sediminis sp. nov., a methanogen from sediments near a
573 submarine mud volcano. Int. J. Syst. Evol. Microbiol. 65, 2141–2147.
574 https://doi.org/10.1099/ijs.0.000233
575 Chouari, R., Le Paslier, D., Daegelen, P., Ginestet, P., Weissenbach, J., Sghir, A., 2005.
576 Novel predominant archaeal and bacterial groups revealed by molecular analysis of an
577 anaerobic sludge digester. Environ. Microbiol. 7, 1104–15.
578 https://doi.org/10.1111/j.1462-2920.2005.00795.x
579 De Baere, L., Mattheeuws, B., 2013. Anaerobic Digestion of the Organic Fraction of
580 Municipal Solid Waste in Europe Anaerobic Digestion of the Organic Fraction of
581 Municipal Solid Waste in Europe-Status, Experience and Prospects. Waste Manag.
582 Recycl. Recover. T.S. Thomé-Kozmiensky Karl J. 3, 517–526.
583 Delbès, C., Moletta, R., Godon, J.J., 2000. Monitoring of activity dynamics of an anaerobic
584 digester bacterial community using 16S rRNA polymerase chain reaction- ingle-strand
585 conformation polymorphism analysis. Environ. Microbiol. 2, 506–515.
586 https://doi.org/10.1046/j.1462-2920.2000.00132.x
587 Dianou, D., Miyaki, T., Asakawa, S., Morii, H., Nagaoka, K., Oyaizu, H., Matsumoto, S.,

2001. Methanoculleus chikugoensis sp. nov., a novel methanogenic archaeon isolated from paddy field soil in Japan, and DNA-DNA hybridization among Methanoculleus species. Int. J. Syst. Evol. Microbiol. 51, 1663–1669. https://doi.org/10.1099/00207713-51-5-1663

Environment and Climate Change Canada, 2020. National Waste Characterization Report [WWW Document]. URL https://publications.gc.ca/collections/collection_2020/eccc/en14/En14-405-2020-eng.pdf (accessed 1.18.22).

EPA, U., 2020. National Overview: Facts and Figures on Materials, Wastes and Recycling | US EPA [WWW Document]. URL https://www.epa.gov/facts-and-figures-about-materials-waste-and-recycling/national-overview-facts-and-figures-materials (accessed 1.18.22).

Faust, K., Raes, J., 2016. CoNet app: inference of biological association networks using Cytoscape. F1000Research 5, 1519. https://doi.org/10.12688/f1000research.9050.2

Geesink, P., Wegner, C., Probst, A.J., Herrmann, M., Dam, H.T., Kaster, A., Küsel, K., 2020. Genome-inferred spatio-temporal resolution of an uncultivated Roizmanbacterium reveals its ecological preferences in groundwater. Environ. Microbiol. 22, 726–737. https://doi.org/10.1111/1462-2920.14865

Gorrie, P., 2019. Toronto Advances RNG Projects | BioCycle [WWW Document]. URL https://www.biocycle.net/toronto-advances-rng-projects/ (accessed 11.17.21).

Guilford, N., 2017. The Anaerobic Digestion of Organic Solid Wastes of Variable Composition | TSpace Repository [WWW Document]. URL https://tspace.library.utoronto.ca/handle/1807/80954 (accessed 11.17.21).

Guilford, N., 2009. A New Technology for the Anaerobic Digestion of Organic Waste | TSpace Repository [WWW Document]. URL https://tspace.library.utoronto.ca/handle/1807/18314?mode=full (accessed 11.17.21).

Guilford, N.G.H., Lee, H.P., Kanger, K., Meyer, T., Edwards, E.A., 2019. Solid-State Anaerobic Digestion of Mixed Organic Waste: The Synergistic Effect of Food Waste Addition on the Destruction of Paper and Cardboard. Environ. Sci. Technol. 53, 12677–12687. https://doi.org/10.1021/acs.est.9b04644

Kanger, K., Guilford, N.G.H., Lee, H.W., Nesbø, C.L., Truu, J., Edwards, E.A., 2020. Antibiotic resistome and microbial community structure during anaerobic co-digestion of food waste, paper and cardboard. FEMS Microbiol. Ecol. 96. https://doi.org/10.1093/FEMSEC/FIAA006

Lai, M., 2019. Bergey's Manual of Systematics of Archaea and Bacteria, Bergey's Manual of Systematics of Archaea and Bacteria. Wiley. https://doi.org/10.1002/9781118960608

Lee, S.H., Park, J.H., Kang, H.J., Lee, Y.H., Lee, T.J., Park, H.D., 2013. Distribution and abundance of Spirochaetes in full-scale anaerobic digesters. Bioresour. Technol. 145, 25–32. https://doi.org/10.1016/j.biortech.2013.02.070

Lee, S.H., Park, J.H., Kim, S.H., Yu, B.J., Yoon, J.J., Park, H.D., 2015. Evidence of syntrophic acetate oxidation by Spirochaetes during anaerobic methane production. Bioresour. Technol. 190, 543–549. https://doi.org/10.1016/j.biortech.2015.02.066

Leven, L., Eriksson, A.R.B., Schnurer, A., 2007. Effect of process temperature on bacterial and archaeal communities in two methanogenic bioreactors treating organic household waste. FEMS Microbiol. Ecol. 59, 683–693. https://doi.org/10.1111/j.1574-6941.2006.00263.x

634 Li, Y., Park, S.Y., Zhu, J., 2011. Solid-state anaerobic digestion for methane production from
635 organic waste. Renew. Sustain. Energy Rev. https://doi.org/10.1016/j.rser.2010.07.042
636 Liu, C., Li, H., Zhang, Y., Si, D., Chen, Q., 2016. Evolution of microbial community along
637 with increasing solid concentration during high-solids anaerobic digestion of sewage
638 sludge. Bioresour. Technol. 216, 87–94. https://doi.org/10.1016/j.biortech.2016.05.048
639 Liu, C.H., Chang, C.Y., Cheng, C.L., Lee, D.J., Chang, J.S., 2012. Fermentative hydrogen
640 production by Clostridium butyricum CGS5 using carbohydrate-rich microalgal
641 biomass as feedstock, in: International Journal of Hydrogen Energy. Pergamon, pp.
642 15458–15464. https://doi.org/10.1016/j.ijhydene.2012.04.076
643 Maus, I., Wibberg, D., Stantscheff, R., Eikmeyer, F.G., Seffner, A., Boelter, J.,
644 Szczepanowski, R., Blom, J., Jaenicke, S., König, H., Pühler, A., Schlüter, A., 2012.
645 Complete genome sequence of the hydrogenotrophic, methanogenic archaeon
646 Methanoculleus bourgensis strain MS2T, isolated from a sewage sludge digester. J.
647 Bacteriol. https://doi.org/10.1128/JB.01292-12
648 Mcintyre, M.S., 2007. City of Ottawa IC&I 3Rs Management Strategy Scoping Document
649 FINAL-APPENDICES.
650 McMurdie, P.J., Holmes, S., 2013. phyloseq: An R Package for Reproducible Interactive
651 Analysis and Graphics of Microbiome Census Data. PLoS One 8, e61217.
652 https://doi.org/10.1371/journal.pone.0061217
653 Mo, S., Kim, B.S., Yun, S.J., Lee, J.J., Yoon, S.H., Oh, C.H., 2015. Genome sequencing of
654 Clostridium butyricum DKU-01, isolated from infant feces. Gut Pathog. 7, 1–7.
655 https://doi.org/10.1186/s13099-015-0055-3
656 Qiao, J.T., Qiu, Y.L., Yuan, X.Z., Shi, X.S., Xu, X.H., Guo, R.B., 2013. Molecular
657 characterization of bacterial and archaeal communities in a full-scale anaerobic reactor
658 treating corn straw. Bioresour. Technol. 143, 512–518.
659 https://doi.org/10.1016/j.biortech.2013.06.014
660 Qiao, W., Puentes Jácome, L.A., Tang, X., Lomheim, L., Yang, M.I., Gaspard, S., Avanzi,
661 I.R., Wu, J., Ye, S., Edwards, E.A., 2020. Microbial Communities Associated with
662 Sustained Anaerobic Reductive Dechlorination of α-, β-, γ-, and δ-
663 Hexachlorocyclohexane Isomers to Monochlorobenzene and Benzene. Environ. Sci.
664 Technol. https://doi.org/10.1021/acs.est.9b05558
665 Qiao, W., Yan, X., Ye, J., Sun, Y., Wang, W., Zhang, Z., 2011. Evaluation of biogas
666 production from different biomass wastes with/without hydrothermal pretreatment.
667 Renew. Energy 36, 3313–3318.
668 R Core Team, 2013. R: A language and environment for statistical computing. R Foundation
669 for Statistical Computing, Vienna, Austria. [WWW Document]. URL
670 https://www.gbif.org/tool/81287/r-a-language-and-environment-for-statistical-
671 computing#citation (accessed 6.27.20).
672 Rintala, J.A., Puhakka, J.A., 1994. Anaerobic treatment in pulp- and paper-mill waste
673 management: A review. Bioresour. Technol. 47, 1–18. https://doi.org/10.1016/0960-
674 8524(94)90022-1
675 Sakai, S., Ehara, M., Tseng, I.C., Yamaguchi, T., Bräuer, S.L., Cadillo-Quiroz, H., Zinder,
676 S.H., Imachi, H., 2012. Methanolinea mesophila sp. nov., a hydrogenotrophic
677 methanogen isolated from rice field soil, and proposal of the archaeal family
678 Methanoregulaceae fam. nov. within the order Methanomicrobiales. Int. J. Syst. Evol.
679 Microbiol. 62, 1389–1395. https://doi.org/10.1099/ijs.0.035048-0

680 Shannon, P., Markiel, A., Ozier, O., Baliga, N.S., Wang, J.T., Ramage, D., Amin, N.,
681 Schwikowski, B., Ideker, T., 2003. Cytoscape: A software Environment for integrated
682 models of biomolecular interaction networks. Genome Res. 13, 2498–2504.
683 https://doi.org/10.1101/gr.1239303
684 Singh, N., Kendall, M.M., Liu, Y., Boone, D.R., 2005. Isolation and characterization of
685 methylotrophic methanogens from anoxic marine sediments in Skan Bay, Alaska:
686 Description of Methanococcoides alaskense sp. nov., and emended description of
687 Methanosarcina baltica. Int. J. Syst. Evol. Microbiol. 55, 2531–2538.
688 https://doi.org/10.1099/ijs.0.63886-0
689 Sowers, K.R., Baron, S.F., Ferry, J.G., 1984. Methanosarcina acetivorans sp. nov., an
690 Acetotrophic Methane-Producing Bacterium Isolated from Marine Sediments. Appl.
691 Environ. Microbiol. 47, 971–978. https://doi.org/10.1128/aem.47.5.971-978.1984
692 Statistics Canada, 2010. Waste Management Industry Survey: Business and Government
693 Sectors.
694 Stoddard, S.F., Smith, B.J., Hein, R., Roller, B.R.K., Schmidt, T.M., 2015. rrnDB: Improved
695 tools for interpreting rRNA gene abundance in bacteria and archaea and a new
696 foundation for future development. Nucleic Acids Res. 43, D593–D598.
697 https://doi.org/10.1093/nar/gku1201
698 Tokuda, G., Mikaelyan, A., Fukui, C., Matsuura, Y., Watanabe, H., Fujishima, M., Brune,
699 A., 2018. Fibre-associated spirochetes are major agents of hemicellulose degradation in
700 the hindgut of wood-feeding higher termites. Proc. Natl. Acad. Sci. U. S. A. 115,
701 E11996–E12004. https://doi.org/10.1073/pnas.1810550115
702 Town, J.R., Dumonceaux, T.J., 2016. Laboratory-scale bioaugmentation relieves acetate
703 accumulation and stimulates methane production in stalled anaerobic digesters. Appl.
704 Microbiol. Biotechnol. 100, 1009–1017. https://doi.org/10.1007/s00253-015-7058-3
705 Van, D.P., Fujiwara, T., Tho, B.L., Toan, P.P.S., Minh, G.H., 2020. A review of anaerobic
706 digestion systems for biodegradable waste: Configurations, operating parameters, and
707 current trends. Environ. Eng. Res. https://doi.org/10.4491/eer.2018.334
708 Větrovský, T., Baldrian, P., 2013. The Variability of the 16S rRNA Gene in Bacterial
709 Genomes and Its Consequences for Bacterial Community Analyses. PLoS One 8, 1–10.
710 https://doi.org/10.1371/journal.pone.0057923
711 Von Klein, D., Arab, H., Völker, H., Thomm, M., 2002. Methanosarcina baltica, sp. nov., a
712 novel methanogen isolated from the Gotland Deep of the Baltic Sea. Extremophiles 6,
713 103–110. https://doi.org/10.1007/s007920100234
714 Wilkins, D., Rao, S., Lu, X., Lee, P.K.H., 2015. Effects of sludge inoculum and organic
715 feedstock on active microbial communities and methane yield during anaerobic
716 digestion. Front. Microbiol. 6. https://doi.org/10.3389/fmicb.2015.01114
717 Wrighton, K.C., Castelle, C.J., Varaljay, V.A., Satagopan, S., Brown, C.T., Wilkins, M.J.,
718 Thomas, B.C., Sharon, I., Williams, K.H., Tabita, F.R., Banfield, J.F., 2016. RubisCO
719 of a nucleoside pathway known from Archaea is found in diverse uncultivated phyla in
720 bacteria. ISME J. 10, 2702–2714. https://doi.org/10.1038/ismej.2016.53
721
722

723

724

725

726

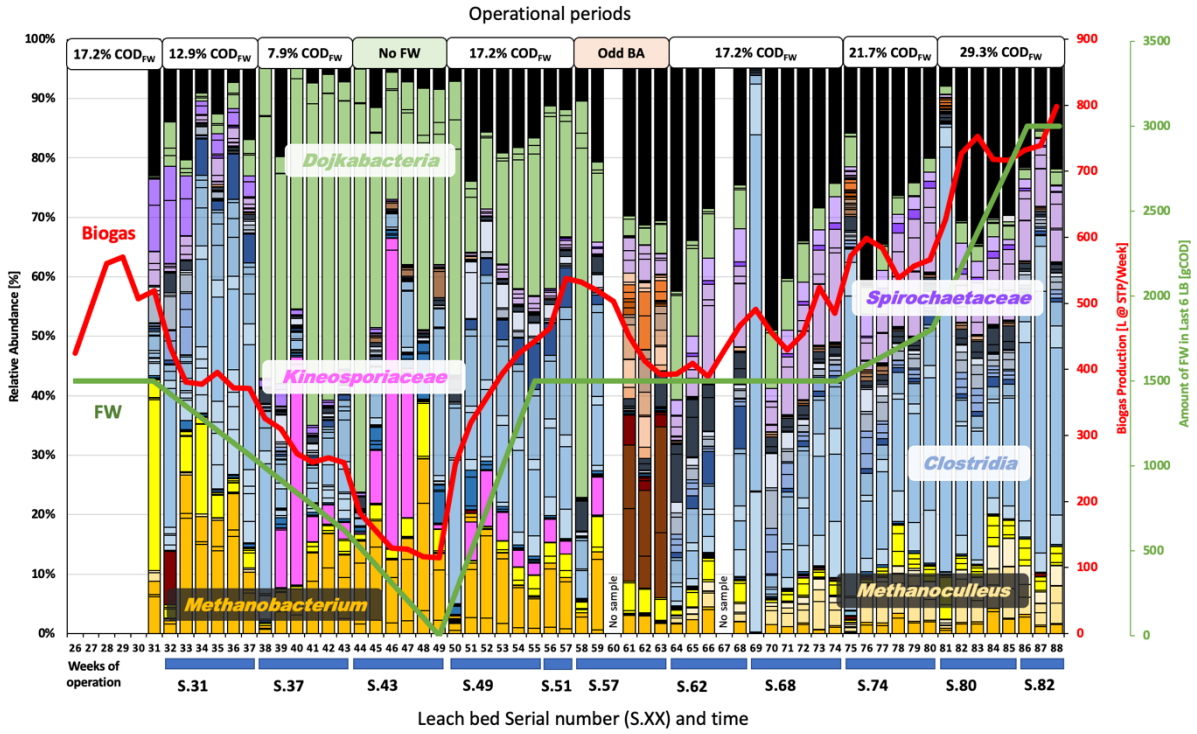

Figure 1. Overview of microbial and process data in Daisy. The relative abundance of microbial community members in weekly leachate samples collected from a given numbered leach bed (stacked bars) is shown in relation to the weekly biogas production rate (red line) and total amount of food waste in the system (gCOD) in the most recent 3 leach beds (green line) from Weeks 26 to 88. The operational periods (top row) show the amount of food waste added to each new leach bed in the corresponding time frame. Odd BA refers to a period with 17.2% COD from FW but a different batch of bulking agent. Shown are the data from sampling the leachate from the first leach bed of a new operational period (referred to as Set 1). Taxa are colour-coded for better visualization. ASVs belonging to *candidate* division Dojkabacteria are shown in green with ASV6777 dominating, particularly as the proportion of food waste dropped to zero. ASVs belonging to *Clostridium* (blue colors) became relatively more abundant when more food waste was present in the system. Archaea are shown in yellow/orange hues. The weekly biogas production appears to correlate well to the amount of food waste added (red and green lines).

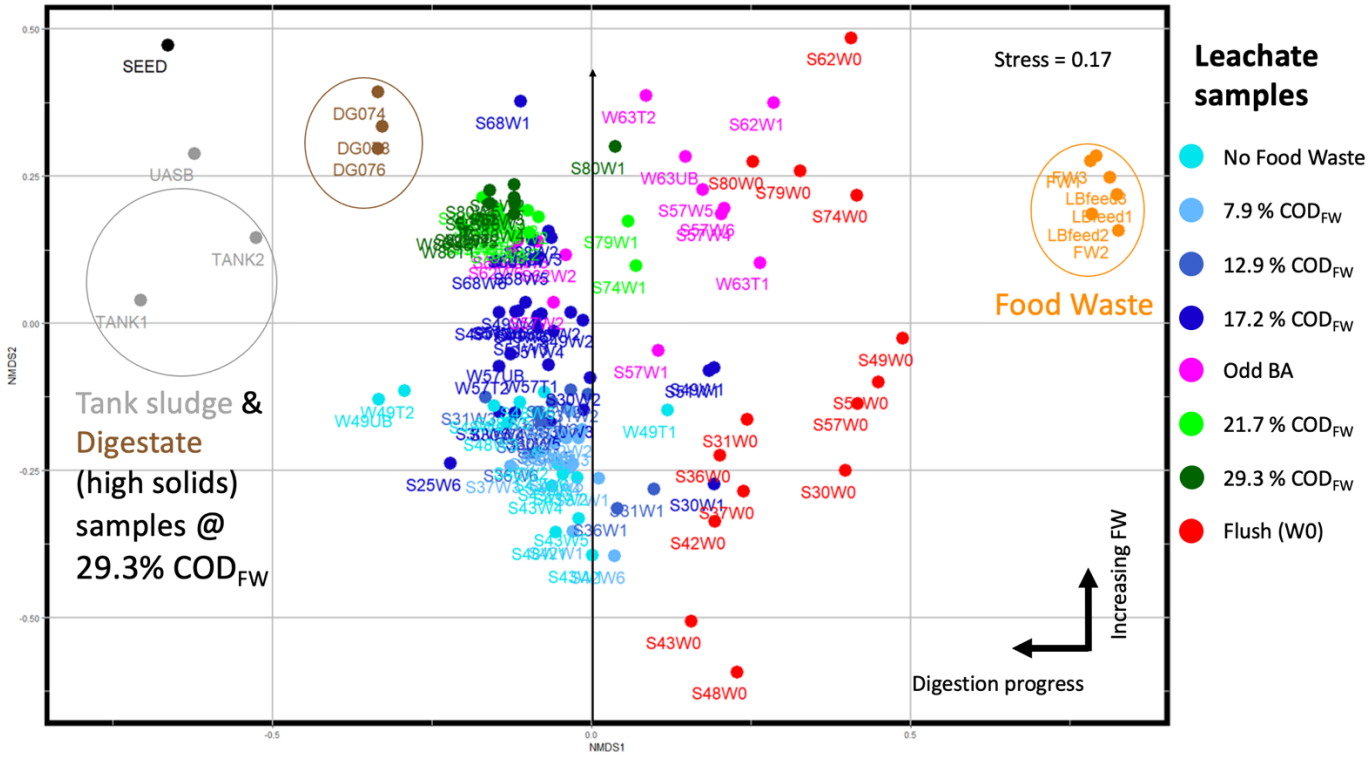

Figure 2. Ordination (NMDS) of Bacterial amplicon sequence data using absolute abundance. Data are color-coded based on amount of FW in the leach bed except for first flush and Odd BA samples. Data from all samples are plotted, including leachate, first flush (W0), food waste (FW) and leach bed feed, digestate (DG), tank sludge, UASB, and original Daisy inoculum (seed). First flush samples (Red) are closest to the food waste and leach bed feed samples (Orange). First flush samples are spread vertically based on the amount of food waste added to the respective leach bed. This was also evident in **Figures S4 and S5**, where number of ASVs with gammaproteobacterial taxonomic assignments were found in both food waste (FW) and **Flush** samples. Samples from leach beds containing less food waste (0 – 12.9 % COD_{FW}, blue tones) clustered below the origin, while those containing more food waste s (21.7 and 29.3 COD_{FW}, green tone) clustered above the origin., with samples containing 17.2% COD_{FW} (Navy) between. Samples collected from leach beds with odd BA (pink) tended to resemble first flush samples, owing to abundant ASVs with gammaproteobacterial assignment.

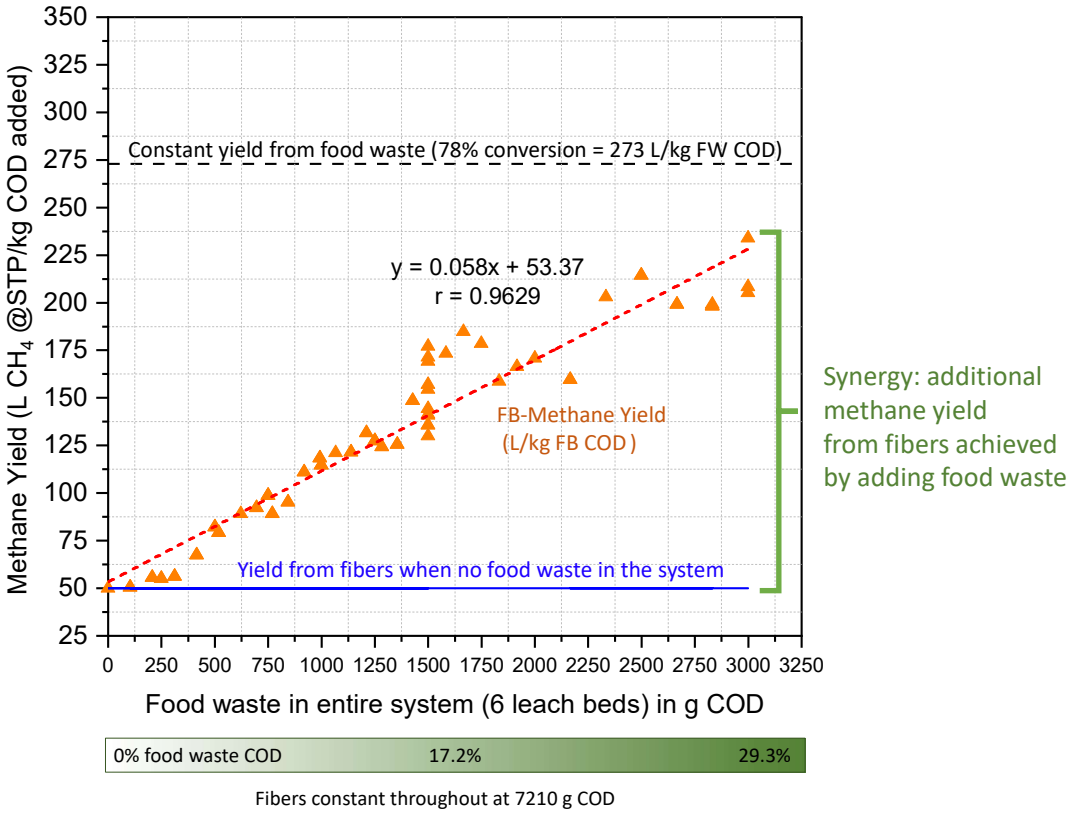

Figure 3. Methane yield from fibers (FB) in L /kg FB_{COD} added as a function of the amount of food waste in the system from all six leach beds. The regression line and Pearson correlation coefficient r show a linear relationship between the amount of food waste (FW) added and FB methane yield. Understanding why food waste contributed to this "synergistic methane" is the main objective of this study. The methane generated from fibers was calculated by subtracting the predicted methane produced from the added food waste (assuming 78% conversion of FW to methane) from total methane produced in the system (see Guilford et al., 2019), and Figure S3 and Table S11 for more information. Each leach bed contained a constant mass of fibers equivalent to 7210 g COD, while Food Waste COD varied from 0 to 3000 gCOD.

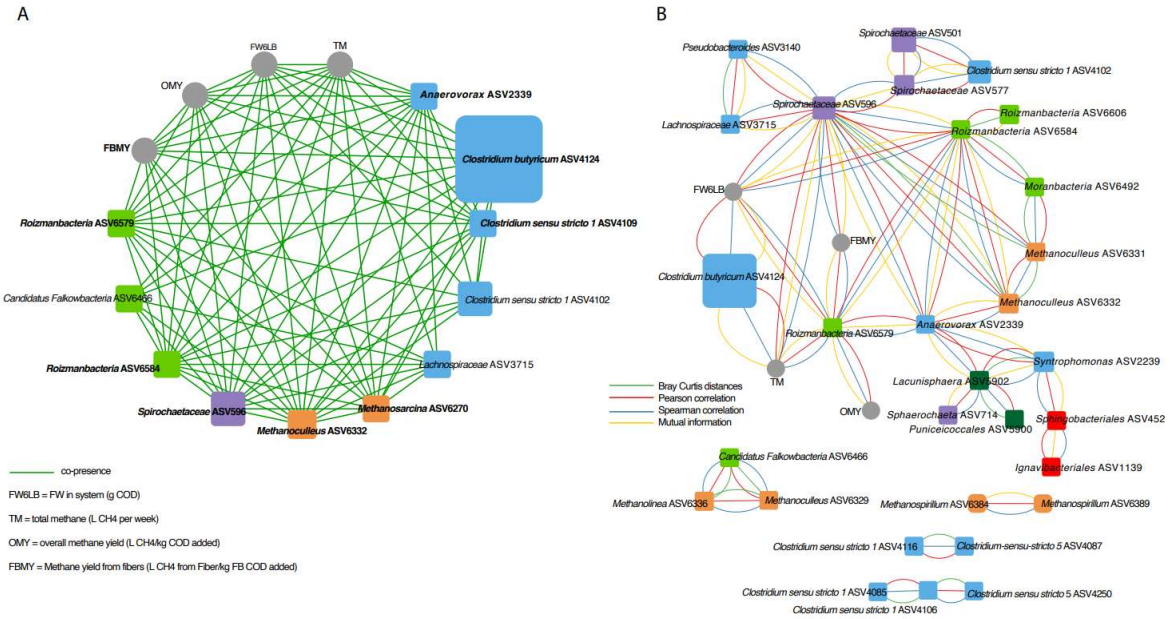

Figure 4. Co-occurrence networks between ASVs and process parameters. A: Subnetwork of the full network shown in Figure S11 including only the eleven ASVs significantly correlated with process metadata. Green edges indicate a positive correlation. **B:** A more stringent network of all ASVs where at least three correlation measures must be significant based on unmerged or individual FDR values. Edges were colored based on test method (green: Bray Curtis distances; red: Pearson correlation; blue: Spearman correlation; yellow: Mutual information). In both panels A and B, process metadata are shown as grey circles and ASVs are shown as squares with size proportional to absolute abundance and coloured according to phylum (red: *Bacteriodetes*, orange: *Euryarchaeota*, blue: *Firmicutes*, green: *Patecibacteria*, purple: *Spirochaetes*, dark green: *Verrucomicrobia)*.

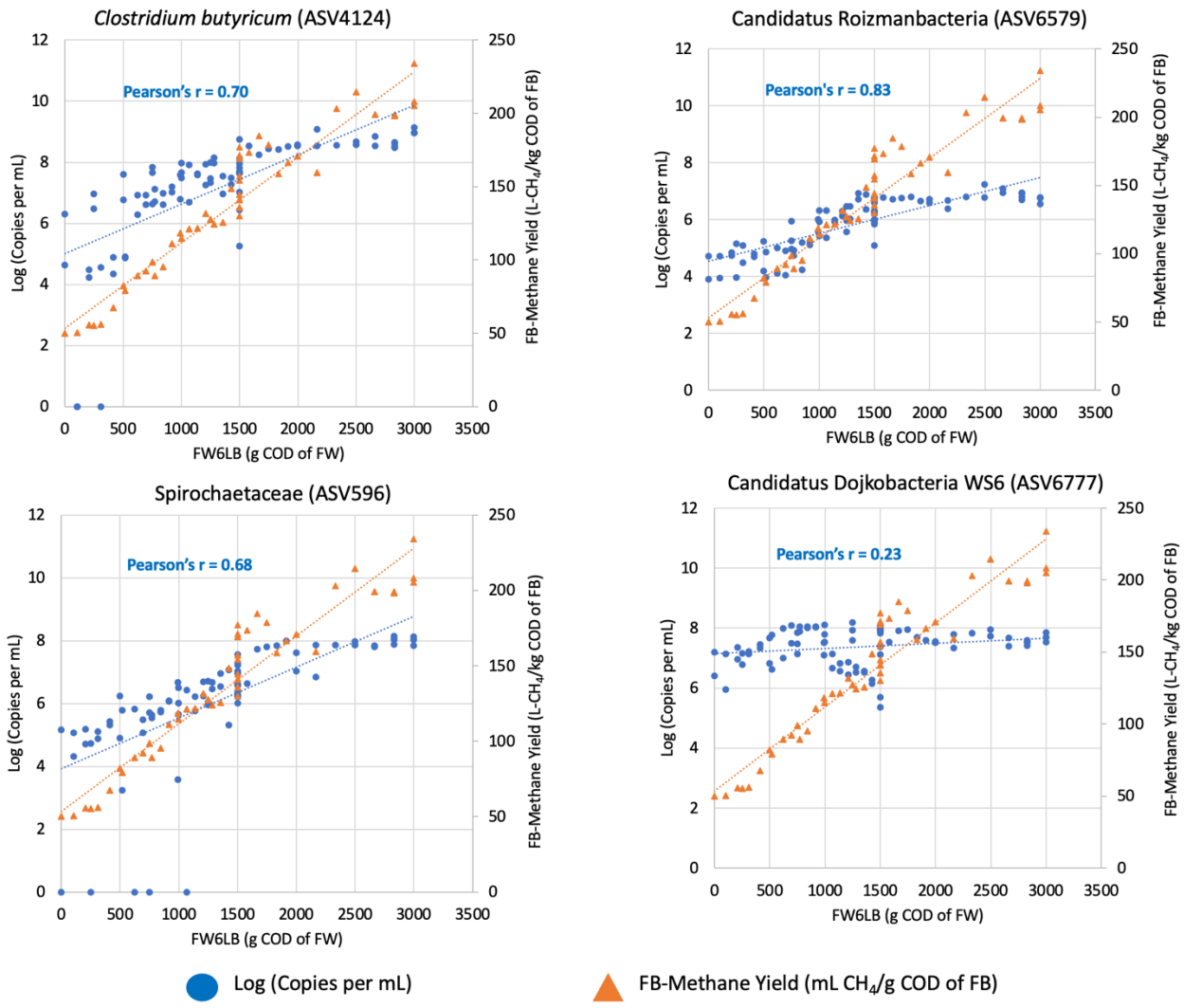

Figure 5. Correlation of microbial phyla with system food waste and methane yield from fibres. The blue dashed line is the regression between log abundance of an ASV (copies per mL) and system food waste (total food waste in 6 leach beds). The orange dashed line is the regression between system food waste and methane yield from fibres. Pearson correlation coefficients are shown for the ASV data. Note that the ASV corresponding to Dojkabacteria (WS6) has very poor correlation. Other notable phyla shown in Figure S12.